Journal of Hazardous Materials 406 (2021) 124299

Contents lists available at ScienceDirect

Journal of Hazardous Materials

journal homepage: www.elsevier.com/locate/jhazmat

Research paper

Visible light photocatalytic degradation of polypropylene microplastics in a continuous water flow system

Abdusalam Uheida [a], Hugo Giraldo Mejía [a,b], Mohamed Abdel-Rehim [a,c], Wael Hamd [d], Joydeep Dutta [a,*]

[a] Functional Materials, Department of Applied Physics, School of Engineering Sciences, KTH Royal Institute of Technology, Hannes Alfvéns väg 12, 114 19 Stockholm, Sweden
[b] Advanced Mining Technology Center (AMTC), Santiago de Chile, Región Metropolitana, Chile
[c] Department of Clinical Neuroscience, Centre for Psychiatry Research, Karolinska Institutet, SE-171 76 Solna, Sweden
[d] Department of Petrochemical Engineering, Faculty of Engineering, Lebanese University, Campus Rafic Hariri, Hadat, Lebanon

ARTICLE INFO

Keywords:
Microplastics
Photocatalysis
ZnO NRs
Microplastics removal
Polypropylene particles

ABSTRACT

Microplastic pollution of water and ecosystem is attracting continued attention worldwide. Due to their small sizes (≤5 mm) microplastic particles can be discharged to the environment from treated wastewater effluents. As microplastics have polluted most of our aquatic ecosystems, often finding its way into drinking water, there is urgent need to find new solutions for tackling the menace of microplastic pollution. In this work, sustainable green photocatalytic removal of microplastics from water activated by visible light is proposed as a tool for the removal of microplastics from water. We propose a novel strategy for the elimination of microplastics using glass fiber substrates to trap low density microplastic particles such as polypropylene (PP) which in parallel support the photocatalyst material. Photocatalytic degradation of PP microplastics spherical particles suspended in water by visible light irradiation of zinc oxide nanorods (ZnO NRs) immobilized onto glass fibers substrates in a flow through system is demonstrated. Upon irradiation of PP microplastics for two weeks under visible light reduced led to a reduction of the average particle volume by 65%. The major photodegradation by-products were identified using GC/MS and found to be molecules that are considered to be mostly nontoxic in the literature.

1. Introduction

Plastics were termed the wonder material in early 1950′s finding applications in wide ranging human activities that has led to an annual production growth of 8.7%, evolving into a US $600 billion global industry (Jambeck et al., 2015). Upon exposure to natural forces like sunlight or waves in water bodies, even larger fragments of plastics degrade into smaller sizes known as microplastics- particles under 5 mm in size including plastic sheets and films in the nanoscale < 1 μm in size. Degradation of plastic depends on the physico-chemical properties of the polymers and environmental conditions like weathering, temperature, irradiation as well as pH. Microplastics and nanoplastics particles in aqueous bodies have aroused increasing concern as a potential threat to aquatic species as well as to human beings. Microplastic particles have been traced in land, water bodies, sea and even in bottled water (Fonseca et al., 2017; Cox et al., 2019). Plastic particles have been found in the food chain, including foodstuffs intended for human consumption wherein in-vivo studies have shown that nanometer sized plastic materials can translocate to organs. Evidence is evolving regarding relationships between micro- and nanoplastics exposure, toxicology, and its consequence to human health (Burns and Boxall, 2018; Redondo-Hasselerharm et al., 2020). For example, plastic particles less than 130 μm in diameter has been found to potentially trigger localized immune responses by translocating into human tissues (Wright and Kelly, 2017).

Microplastic particles are used in a number of cosmetic and personal care products, including washing liquids, soaps, facial and body scrubs, toothpaste, and lotions. Most of the microplastics used in personal care products are generally polyethylene (PE) and polypropylene (PP) which can end up in municipal wastewater treatment plants (WWTPs) and ultimately in the environment since present wastewater treatment plants are designed to remove organic matter but not microplastics. Tertiary treatment processes commonly used for the removal of microplastics from effluents in WWTPs utilize ultrafiltration (UF),

* Corresponding author.
E-mail address: joydeep@kth.se (J. Dutta).

https://doi.org/10.1016/j.jhazmat.2020.124299
Received 6 August 2020; Received in revised form 28 September 2020; Accepted 14 October 2020
Available online 17 October 2020

coagulation, reverse osmosis (RO), and Membrane bioreactor (MBR) (Chang, 2015; Fendall and Sewell, 2009; Murphy et al., 2016). Although removal efficiency of 90–99% has been reported, microplastics of 20–300 μm in size still have problems to be removed (Browne et al., 2011; Enfrin et al., 2019; Sol et al., 2020; Talvitie et al., 2017) and microplastics in discharged water up to 0.25 particle/L has been detected (Murphy et al., 2016). Furthermore, the sludge as residuals of WWTPs processes containing microplastics may be used as agricultural fertilizers that subsequently finds its way into the groundwater (Bratovcic, 2019).

Over the course of time, several technologies have been implemented to manage the plastic menace, including, but not limited to, thermal degradation, incineration, landfills and ozonation (Davis et al., 1962; Arutchelvi et al., 2008; Canopoli et al., 2020). However, these technologies utilize large amount of energy and are often very expensive. Recent methods investigated for the treatment of microplastics waste are biodegradation and photocatalysis. Biodegradation of microplastics can be achieved by microbes producing enzymes that break the macromolecules into smaller fragments which can potentially lead to complete mineralization (Silva et al., 2018). For example, biodegradation of PP microplastics using *Bacillus cereus* and *Bacillus gottheilii* bacteria has been investigated and it has been found that long exposure time is needed in order to achieve high removal efficiency (Auta et al., 2017).

Visible light photocatalysis is a promising environmentally friendly, low-cost and efficient process that is capable of mineralizing a wide variety of organic pollutants into H_2O and CO_2 (Nakata and Fujishima, 2012). This process offers advantages such as the utilization of sunlight as a clean energy source, high degradation efficiency, and the generation of harmless by-products. It is based on the use of suitable wide bandgap metal oxide semiconductor materials such as titania (TiO_2) or zinc oxide (ZnO), that upon interaction with light give rise to the formation of different reactive species. When ZnO, TiO_2 or similar semiconductors are excited by light sources with an energy greater than their inherent bandgap, charge separation is created in the form of free electrons, excited from their valence band positions into the conduction band. This excitation simultaneously leads to a hole formation in the valence band. Both free electrons and holes react with H_2O, OH^- and O_2 adsorbed in the surface of the semiconductor to generate reactive oxygen species (ROS) such as hydroxyl ($OH^{\cdot}$) and superoxide (O_2^{-}) radicals. These species initiate the polymer degradation process, leading to chain scission and complete mineralization into H_2O and CO_2 (Zhao et al., 2007). The photocatalysis process is described by the following equations:

$$Photocatalyst \xrightarrow{h\nu} h^+ + e^- \quad (1)$$

$$h^+ + H_2O \rightarrow OH^{\cdot} \quad (2)$$

$$e^- + O_2 \rightarrow O_2^{-\cdot} \quad (3)$$

$$Organic\ pollutant + ROS \rightarrow CO_2 + H_2O \quad (4)$$

In this work, the photocatalytic material tested for the degradation of microplastics was defect-engineered ZnO, due to its low price, high redox potential, nontoxicity, and environmentally friendly features (Baruah et al., 2008; Bora et al., 2017). ZnO is listed in a "generally recognized as safe" (GRAS) material by the Food and Drug Administration (FDA) and is an essential element for human physiological activities (EFSA, 2015). Due to its tailorable defect chemistry, ZnO has been widely used for both UV light and visible light degradation of organic molecules (Al-Sabahi et al., 2016, 2017, 2018; Bora et al., 2016). Moreover, it was recently validated for degrading microplastic residues by our group (Tofa et al., 2019a, 2019b). Thus, based on multiple factors like visible light absorption capacity (thus using sunlight for degradation would be viable) (Baruah et al., 2008, 2010; Bora et al., 2017), low degree of toxicity to marine and human life (Dobretsov et al., 2020), flexibility to be grown on various substrates at low temperatures (100 °C) (Baruah and Dutta, 2009), high electron mobility due to its single crystalline wurtzite structure, and appropriate defected engineering possibilities to enhance visible light absorption, ZnO was considered to be a suitable candidate for the degradation of commercial microplastic particles.

In the literature, nanocomposite films of TiO_2 (El-Dessouky and Lawrence, 2010; García-Montelongo et al., 2014; Nabi et al., 2020; Verma et al., 2017), N-TiO_2 (Ariza-Tarazona et al., 2019; Llorente-García et al., 2020), ZnO (Tofa et al., 2019a, 2019b; Zhao and Li, 2006), Pt-ZnO (Tofa et al., 2019a, 2019b), C-TiO_2 (Kamrannejad et al., 2014) as well as C,N-TiO_2powders (Ariza-Tarazona et al., 2020) have been reported for the removal of microplastics particles and fragments. Although reasonable degradation efficiencies were reported, yet these systems have some limitations such as: (i) the experimental setup used does not reflect the real situation of the treatment of microplastics dispersed in wastewater effluents; (ii) recovery of the photocatalytic powder after photodegradation process using filtration adds additional needs for membrane separation often adding cost. Herein, we propose a novel strategy for the removal of microplastics using glass fiber substrates to trap the low density microplastics particles while acting as a supporting substrate for the photocatalyst. This approach may represent a good alternative, especially for the treatment of WWTPs effluents containing microplastics prior its release to the environment.

To the best of our knowledge the visible light photocatalysis of microplastics particles and in water flow system in order to mimic the real situation as in water treatment facilities and wastewater treatment plants has not been reported. Therefore, this work investigates the photocatalytic degradation of microplastics spherical particles suspended in water by visible light irradiation of ZnO NRs immobilized onto glass fibers substrates (photocatalyst) in a flow through system. PP microplastics with an average particle size of 154.8 ± 1.4 μm was selected as pollutant model because it is a major aquatic pollutant due to its lower density than water. Thus PP has the potential of being mistaken as a feed even by smaller aquatic animals and fishes which search for food on surface of water complicated by the fact that the half-life of PP is a few hundred years. Furthermore, the photocatalytic activity of ZnO NRs is evaluated by considering the evolution of the carbonyl index parameter and the main water soluble by-products formed during the degradation process was identified using GC-MS.

2. Experimental

2.1. Materials

PP microplastics were provided by PPPolymer AB, Sweden (ELTEX® P HV001PF polypropylene supplied in the form of un-stabilized free flowing powder. Melt flow rate = 10 g/10 min, density = 905 Kg/m^3, Flexural modulus = 1600 MPa). The substrate material, glass fibers (~16 μm thick strands), was purchased from Sigma Aldrich. Zinc nitrate hexahydrate ($Zn(NO_3)_2 0.6H_2O$; Sigma Aldrich), hexamethylenetetramine ($(CH_2)_6N_4$; Sigma Aldrich), zinc acetate dehydrates ($Zn(CH_3COO)_2 0.2H_2O$; Sigma Aldrich) were used as received without further purification. High purity water with a resistivity of 18 MΩ·cm was used throughout all the experiments.

2.2. Fabrication of the nanocoating material

The synthesis of ZnO NRs immobilized on glass fibers is described elsewhere (Bora et al., 2017; Baruah et al., 2010). Briefly, a thin layer of ZnO nanocrystallite seeds were deposited on glass fibers (~1 g) substrates pre-heated to 350 °C, by spraying 20 mL of 10 mM solution of zinc acetate dehydrate in isopropanol with a flow rate of ~1 mL/min. Hydrothermal growth of ZnO NRs was carried out by placing the seeded glass fiber substrates in a chemical bath containing equimolar concentrations (10 mM) of zinc nitrate hexahydrate and hexamethylenetetramine, at 90 °C for a total of 9 h, where the precursor solution was changed twice, as described elsewhere (Baruah and Dutta, 2009; Baruah

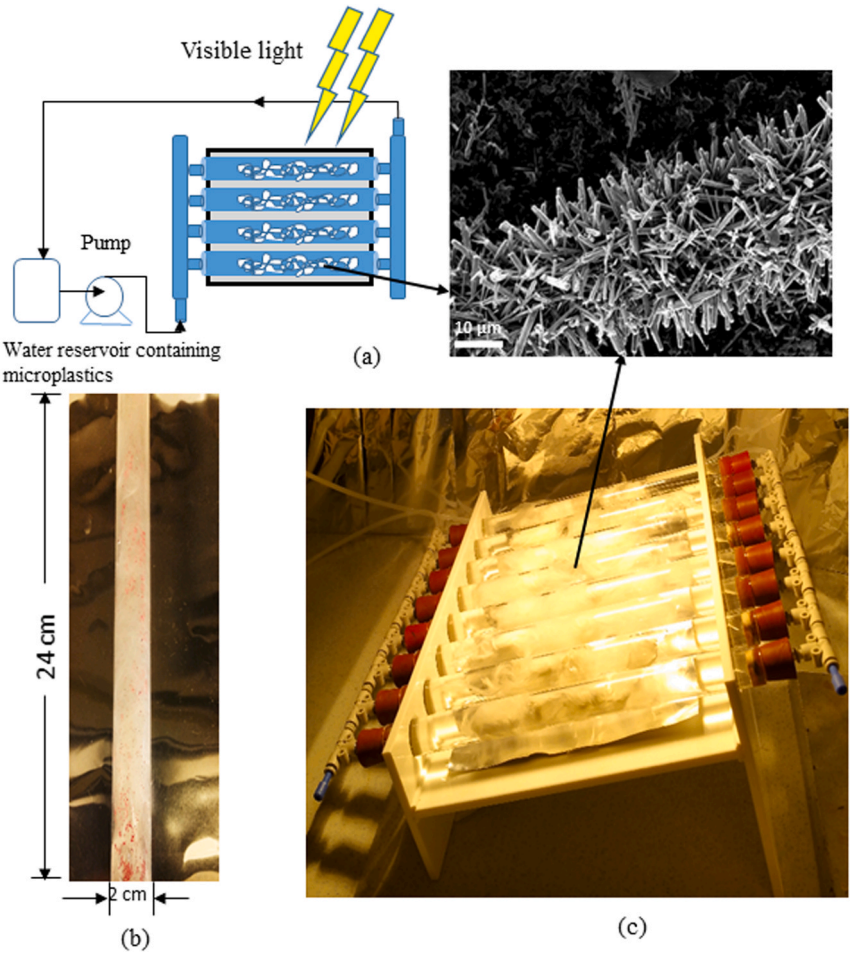

Fig. 1. (a) Schematic diagram of the photocatalytic reactor showing the ZnO nanorod coated glass fiber inserts, (b) the polymer distribution shown inside the photocatalytic reactor (polymer particles were colored for imaging using glyceride, a pyrrolidone, a resin and a colorant to attach on polymer microparticles). (c) optical image of the photocatalytic module fabricated for this work.

and Dutta, 2009). The as grown ZnO NRs were thoroughly washed with deionized (DI) water and annealed in an atmospheric furnace at 350 °C for 1 h (Bora et al., 2017; Promnimit et al., 2012; Al-Saadi et al., 2017).

2.3. Design of the photocatalytic reactor

The photocatalytic reactor used in this work evolved from our earlier research as shown in Fig. 1 (Baruah et al., 2012). The photo-reactor panel is made of transparent soda-lime glass tubes (8 tubes with diameter = 2 cm, and length = 24 cm) placed on top of a reflector. The reflector was used to improve the efficiency of photon absorption by the photocatalyst by allowing at least a double pass of light through the catalyst. The reflector illuminates the bottom of the nanocoated material (photocatalyst) so that the illuminated surface area of the photocatalyst is improved. Mirror polished aluminum sheets of 300 μm thickness were used as reflectors. Polyethylene pipes and valves were used in the photo-reactor due to the robustness of these materials. Water was passed along the tubes to a reservoir using a peristaltic pump, permitting a turbulent flow of water inside the photo-reactor. The photo-reactor tubes were made of glass to enhance the light transmission and to avoid any possible contamination (if plastic tubes were used) during photocatalytic degradation process. The reflector and glass tubes were placed on a frame tilted at 30° angle in order to enhance the illuminated surface area of the photocatalyst. However, to ensure an effective dissolution of oxygen in the aqueous solution, turbulent regime was established in the re-circulatory continuous flow device. The photocatalyst (~ 60 mg ZnO NRs coated on 10 g glass fiber substrates) was loaded into the glass tubes of the reactor panel and kept inside using stopper at either ends of the tube. Each glass tube (total of 8 tubes) of the reactor panel was loaded with about 7.5 mg of ZnO NRs coated on ~ 1.3 g glass fiber substrates.

2.4. Photodegradation experiments

A known amount of PP microplastic particles (~ 70 mg, ~ 10^4 particles) was suspended in highly pure water with a resistivity of 18 MΩ·cm in a recipient (water reservoir). Water containing microplastic particles of concentration of 10^4 particles/liter was then circulated through the photoreactor using peristaltic pump (model Masterflex No. 7521–47, Cole-Parmer, USA) at a flow rate of 300 mL/min. The nanocoated glass fibers materials were subjected to visible light irradiation using a tungsten-halogen lamp of 120 W (ES-HALOGEN) with light intensity of about 0.6 SUN (60 mW/cm^2) measured by a power meter (IM-750) at a distance of 20 cm from the light source. Samples of the microplastics particles were extracted from the glass fibers at fixed intervals of time during photoirradiation and the particles were air dried prior to further analysis. For the microplastics particles to degrade, one important criterion should be that they are in close proximity to ZnO NRs photocatalysts, and the microplastics particles are uniformly distributed in the glass fibers matrix containing the photocatalyst. Therefore, in this work the distribution of PP microplastics within the ZnO NRs coated glass fibers matrix was tested. For this purpose, a marker technique using a permanent color was implemented to optimize the distribution of the polymeric particles in the nanorod coated matrix. We have used red color commercial permanent marker to color the PP

microplastics particles (originally in white color) for imaging purposes. The ingredient of the permanent marker is glyceride, a pyrrolidone, a resin and a colorant to attach on polymer. The microplastic particles were found to distribute uniformly into the photocatalytic reactor and collect thoroughly on the glass fiber inserts (Fig. 1b).

2.5. Characterization

2.5.1. Differential scanning calorimetry (DSC) and thermogravimetric analysis (TGA)

DSC measurements were carried out in a Q2000 instrument (TA Instruments, USA) to investigate the crystallization behaviour. The heating and cooling rates used were the same for all the measurements (10 K/min). The crystallinity of the polymeric samples was estimated from the DSC data. Thermogravimetric Analysis (TGA) was carried out with TGA-Q500 (TA Instruments, USA) at a heating rate of 10 °C/min over a temperature range of 30–600 °C under continuous nitrogen flow.

2.5.2. Fourier transform infrared coupled attenuated total reflectance (FTIR–ATR)

The FTIR–ATR (Nicolet iS10, Thermo Fisher Scientific, USA) was used to quantify the carbonyl contents of PP microplastics from infra-red spectra ranging from 4000–650 cm^{-1} with signal averaged over 32 scans at a resolution of 4 cm^{-1}. Carbonyl groups were detected in the broad infrared region at 1550–1850-cm^{-1} for oxidized PP, and the peak at 2721 cm^{-1}, which is associated with CH bending and CH_3 stretching, was used as reference. The carbonyl index (CI) therefore is expressed by

$$CI = \frac{A_{C=O}}{A_{2721}} \quad (5)$$

where $A_{C=O}$ is the area of the carbonyl absorption band (1550–1850 cm^{-1}), and A_{2721} is the area of the reference band in the range of 2700–2750 cm^{-1}.

2.5.3. Scanning electron microscopy (SEM) and optical microscope analysis

SEM analysis was carried out using scanning electron microscope (GEMINI Ultra 55, Carl Zeiss AG, Germany). SEM was used to confirm the attachment of ZnO NRs to the glass fibers and the PP microplastics particles morphology analysis. After photodegradation, the PP particles were extracted from the glass fibers substrates and dried in air prior to loading in the scanning electron microscope. PP microplastic particles were placed on conductive carbon tapes which was stuck on a SEM sample stub. Then the stub with mounted PP microplastics particles were coated by sputtering a thin layer of gold (JFC-1100, JEOL Nordic AB) to avoid charging during electron microscopy. Sputtered gold was deposited for 2 min at 1.2 kV and 10 mA.

Furthermore, the diameter of PP microplastics particles and glass fibers was measured using a standard optical microscope. The microplastics particle size was measured using optical microscope (Leica DML, Leica Microsystems, Wetzlar, Germany) connected to a digital camera which captured the images. After photodegradation, the PP particles were extracted from the glass fibers substrate and then dried in air before characterization using optical microscope. The size distribution was determined using image analysis software (ImageJ, version k 1.45). The average microplastic particles size was estimated from a sample of 400 particles. Based on the obtained particle sizes, the particle volume reduction percentage was calculated as follows;

$$\text{Particle volume reduction percentage} = \left(\frac{\textit{initial volume of PP particle}}{\textit{initial volume of PP particle} - \textit{volume of PP particle after irradiation}}\right) \times 100 \quad (6)$$

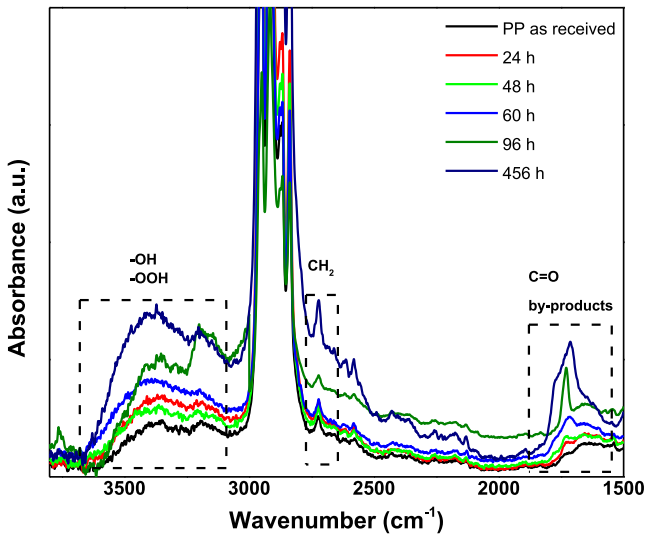

Fig. 2. FT–IR spectra of PP microplastic particles before and after 24 h, 48 h, 60 h, 96 h and 456 h of visible light irradiation highlighting the most prominent peaks from –OH, –OOH, CH_2 and C=O groups.

2.5.4. Gas chromatography–mass spectroscopy (GC/MS)

GC/MS was used to attribute the degradation by-products. Water samples at different irradiation intervals were collected and analysed using GC/MS. Prior to the GC/MS analysis, water samples were pretreated using solid phase extraction (SPE) technique. To extract polar and non-polar substances, two types of sorbents were investigated including, crosslinked poly(styrene divinylbenzene) (ENV+) and silica-based (Si-C18). The ENV + sorbent showed good selectivity and high capacity compared to C18 sorbent. This is in good agreement with earlier published data that the polymeric sorbent (PS) such as polystyrene has greater capacity per gram than silica based sorbent (Si-C18) and it is able to adsorb a wider range of analytes from polar to nonpolar (Ashri and Abdel-Rehim, 2011). The SPE columns (100 mg) were activated with 1 mL methanol followed by 1 mL deionized water (MilliQ, resistivity= 18 MΩ). 20 mL of water samples were loaded slowly through the SPE column. The extracted substances were then eluted with 10 mL methanol. The collected samples were then allowed to evaporate using nitrogen gas and the volume was reduced from 10 to 2 mL. The studied samples and blank water samples were treated similarly. However, as PS sorbents work reasonably well, we have attempted to standardize a simple way to identify the end products obtained during the photodegradation process. Higher peak response of the extracted compounds was observed using ENV + phase compared to Si-C18. The GC/MS system was an HP 6890-Plus gas chromatograph fitted to a mass selective detector model 5973 (Agilent, USA) and fused silica capillary column (30 m x 0.25 mm) coated with CP-SIL 8CB (0.5 μm film thickness). Helium was used as a carrier gas (AGA, Stockholm, Sweden). The GC oven was held at 80 °C for 5 min and then it was increased to 270 °C (50 °C/min) and then held at 270 °C for 3 min. The temperatures of the transfer line and MS ion source were 280 and 230 °C, respectively. The electron impact ionization was set at 70 eV during all the measurements. 2 μL of the extracted sample were injected into the GC injector (injector temperature was 250°C) and MS-EI was used for the screening of the degradation products in the range of *m/z:* 30–550.

3. Results and discussion

3.1. Characterization of PP and the nanocoating material

Scanning electron micrographs of ZnO NRs and the glass fibers substrates are shown in Figure 1S "Supplementary Material". The glass

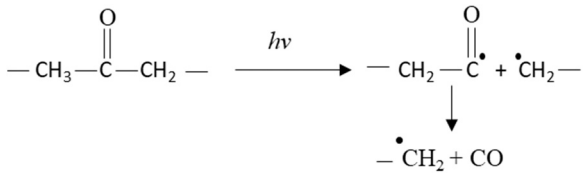

Fig. 3. Typical Norrish I mechanism (Torikai et al., 1983).

fibers supports of diameter ~16 μm were coated with ~1.6 μm long and ~200 nm wide ZnO NRs. The surface area of a typical 2 μm ZnO NR is calculated to be ~1.5×10^3 nm^2. With the total number of rods estimated to be ~8×10^{12}; the total surface area of ZnO NRs in the reactor is calculated to be ~120 cm^2. In a similar way the total surface area of the glass fibers (coated substrate) was estimated to be around 300 cm^2. The average particle size of the as received PP polymer (estimated from a sample of 400 particles) measured using optical microscope was found to be 154.8 ± 1.4 μm. Figure 2S "Supplementary Material" shows the optical image of the as received PP microplastics and the particle size distribution.

3.2. Visible light photocatalysis of PP microplastics

3.2.1. Fourier transform infrared spectroscopy analysis

The obtained FTIR spectra for PP microplastics after photodegradation under visible light irradiation at different intervals of time is shown in Fig. 2. Photo-oxidation of PP has been identified and quantified by the presence of strong absorption bands assigned to carbonyl (C=O) and hydroxyl/hydroperoxyl (–OH, –OOH) groups. Absorbance in the region of 1725 cm^{-1} and 3500 cm^{-1} indicate the presence of carbonyl and hydroxyl groups, respectively, while the absorbance peak at 2722 cm^{-1} is attributed to the angular molecular vibrations in CH and axial molecular vibrations in CH_3 (de Carvalho et al., 2013).

As shown in Fig. 2, after 60 h of photo-irradiation, the carbonyl peak shows an asymmetric broad and medium intensity band between ~1750–1700 cm^{-1}. Correspondingly during the same period, the band corresponding to the stretching mode of the hydrogen-bonded hydroxyl group of alcohol and peroxide between ~3300–3500 cm^{-1} grows considerably, suggesting that photo-oxidation of PP is dominated by the formation of hydroxyl groups more than carbonyl by-products during this period. After 96 and 456 h of irradiation, the concentration of the carbonyl groups and the per-hydroxyl bands are exceedingly high which can be attributed to the formation of large amounts of per-hydroxyl species. This is plausible since the initial oxidation products and their formation is preferential due to Norrish (I) mechanism, until more advanced oxidation takes place (García-Montelongo et al., 2014; Verma et al., 2017; Aslanzadeh and Haghighat Kish, 2010; Ohtani et al., 1989; White et al., 2006; Yang and Martin, 1994). Norrish type I mechanism (Fig. 3) describes the photochemical cleavage of aldehydes and ketones into two free radical intermediates. Norrish I mechanism leads to chain scission and formation of radicals that might initiate the photooxidation process (Rånby, 1989).

Finally, carbonyl products such as esters or carboxylic acids are generated, as shown by the intense and broader carbonyl band in samples photo-irradiated for 456 h. It can be noted that the formation of hydroxyl and carbonyl groups takes place simultaneously during the photodegradation process. It can be argued that an increase in exposure time causes an increase in the intensities of both the carbonyl band and the hydroxyl band, as shown in Fig. 2. Therefore, the major oxidation products include hydrogen-bonded hydroperoxides and carbonyl compounds.

The carbonyl and reference bands used for the determination of carbonyl index (CI) during PP microplastics photodegradation are shown in Figure 3S "supplementary material". The CI values obtained

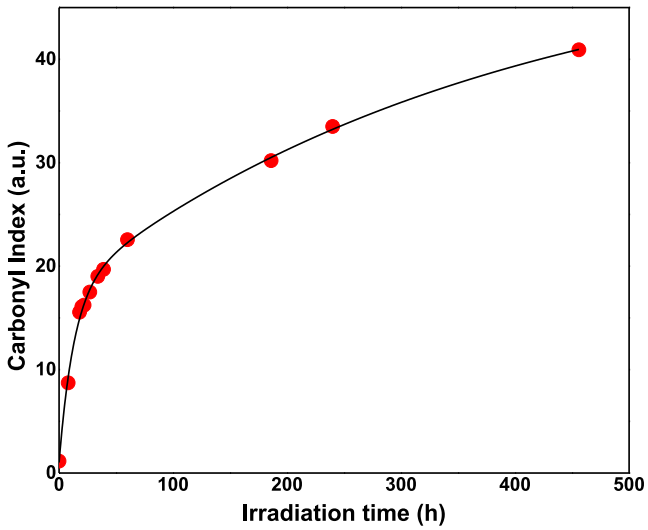

Fig. 4. Carbonyl index (CI = $\frac{A_{C=O}}{A_{2722}}$), where $A_{C=O}$ is the area of the carbonyl absorption band (1550–1850 cm^{-1}) and A_{2722} is the area of the reference band (3300–3500 cm^{-1}) during photodegradation of PP as a function of the irradiation time.

from the analysis of FTIR spectra is used to characterize the degree of oxidation of PP microplastics. The results obtained (Fig. 4) show a continuous increase in carbonyl absorption for PP microplastics with increasing duration of light exposure. Fast kinetics of the evolution of carbonyl, hydroxyl and/or hydroperoxides groups is observed, in which relatively high CI of ~9 can be obtained at short exposure times of 8 h. The photodegradation rate achieved in this study is much faster than what was reported in the literature for the photodegradation of PP films and fibers (Aslanzadeh and Haghighat Kish, 2010; White et al., 2006; Yang and Martin, 1994; Rabello and White, 1997; Torikai et al., 1983). This important enhancement might be attributed to the structure and morphology of the nanocoating material (photocatalyst) used in this study. In addition, the forced fluid flow pattern within the prototype reactor used in this work allows good interaction between the photocatalyst surface and the microplastics and could be effective at enhancing the degradation rate and process (Ariza-Tarazona et al., 2020).

In the literature, the CI values after photodegradation of PP films under UV light exposure was reported to be in the range of 0.2–25 for exposure times from 6 to 4200 h (Rabello and White, 1997; Torikai et al., 1983). In this work, the carbonyl index versus irradiation time showed high CI values (>40) that indicate significant degradation efficiency as it was achieved over a relatively short period of exposure time (456 h). The CI diagram also shows a continuous increasing relation between the irradiation time and the evolution of carbonyl species. The coefficient grows more than 20 times compared to the as received PP microplastics after 456 h of photo-irradiation. Furthermore, photo-enhanced dissolution of ZnO NRs examined using inductively coupled plasma optical emission spectroscopy (ICP-OES) was found to be less than 0.5% (within the level of experimental limits) after 456 h of exposure to visible light (determined from the treated water).

3.2.2. Thermal analysis

The thermal decomposition profiles from thermogravimetric (TG) measurements shows clear differences between samples of PP microplastics after different lengths of exposure to visible light (Figure 4S "supplementary material"). Furthermore, the thermal properties of the irradiated polymer were analysed by DSC heat ramp (Fig. 5). The process of photodegradation of PP microplastics induces a shift in the melting point to lower temperatures with an increasing shift for samples treated for a longer time. This might be attributed to the reorganization

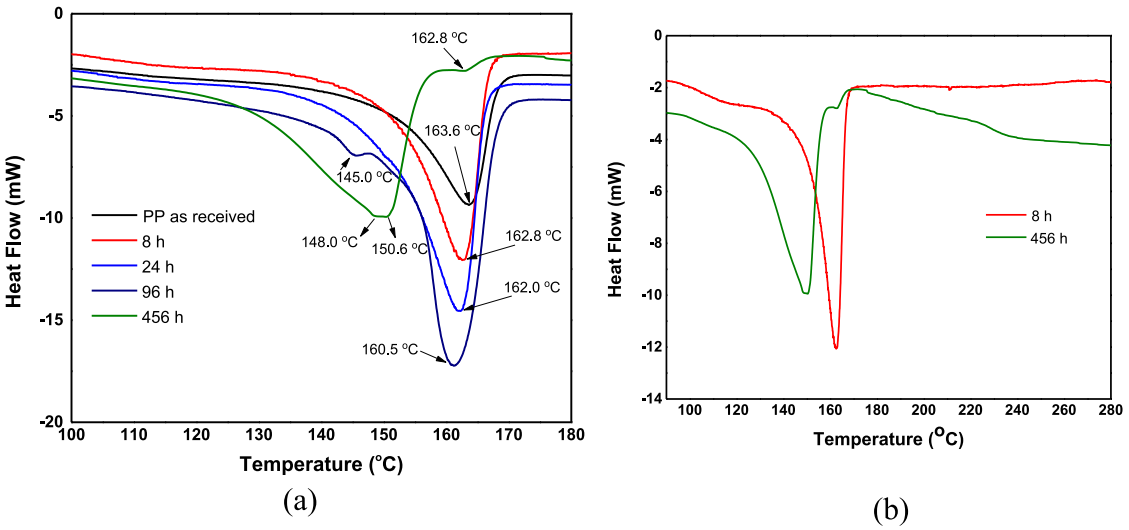

Fig. 5. (a) Differential scanning calorimetric (DSC) analysis of PP microplastics after photodegradation for different periods of time, and (b) DSC profile in the temperature range of 180–280 °C.

of macromolecular chains into structures that exhibit lower melting point, leading to the shift of the main endothermic peak (162 °C) (Rouillon et al., 2016). With the evolution of the degradation, an additional peak in the region of 145–150 °C was found to appear, and in samples treated for longer periods of time (456 h), this peak is even more prominent than the peak observed at 160 °C that correspond to the long chains of the as received PP microplastics. This phenomenon is consistent with the chain scission mechanisms suggesting that prolonged photocatalytic treatment leads to the degradation of the polymeric chains.

Upon photocatalytic treatment for 456 h, the main peak, T_m, the temperature ranges of melting (start 130 °C- finish 155 °C) broadens, suggesting an increase in the mobility of the chains, which is consistent with a mechanism that involves chain scission and generation of lower molecular mass by-products like Norrish I transformations (Aslanzadeh and Haghighat Kish, 2010). In addition, after 456 h of photo-irradiation, an endothermic phenomenon can be observed at high temperatures (continuous decreasing heat flow between 180 and 280 °C) in the DSC profile (Fig. 5b). This behaviour suggests an early start of degradation by-products and short chains as confirmed by TGA analysis (Figure 4S "supplementary material"). This phenomenon has not been observed in microplastic particles treated for shorter exposure times.

3.2.3. Microplastics morphology analysis

Photodegradation of PP microplastics was also investigated by SEM analysis. Fig. 6 shows SEM micrographs of PP microplastics photo-irradiated for different periods of time. The visible changes in the surface microstructure of the microplastic particles occur due to a combination of the removal of the photodegradation by-products, restructuring of the surface amorphous content, and the increase of the crystalline fractions leading to shrinkage of surface layer and the formation of cracks and cavities (Nabi et al., 2020; Verma et al., 2017). The presence of surface cracks (some are marked with circles) and cavities (some are marked with squares) would increase the extent of degradation by providing a pathway for oxygen to penetrate deeper into the sample and enhance photooxidation. The size of the cavities and its density increase constantly for longer photocatalytic treatment times. The formation of cavities could also be due to the removal of the volatile degradation products from the polymer particle surfaces.

Furthermore, the particle size of PP microplastics before and after exposure was measured. The measured particle size and the size distribution averaged over 400 particles at different exposure time are summarized in Table 1. PP microplastics particle size reduced gradually as the irradiation time was increased which is expected due to the degradation of polymeric chains and loss of degradation products to water.

The percentage reduction of PP microplastics particle volume as a function of irradiation time is shown in Fig. 7. Over 65% volume reduction of PP microplastics could be obtained after 456 h of visible light exposure during the photocatalytic degradation process. Elimination of the by-products formed because of photodegradation provides unoccupied spaces for the reduction of the particle volume and depletion in the surface layer as observed from the SEM images of the degraded microplastics (Fig. 6). Similar results were reported for the photo-oxidation of PP fibers exposed to UV irradiation (Aslanzadeh and Haghighat Kish, 2010).

3.2.4. Characterization of photodegradation by-products

The GC/MS technique was used in order to identify the main water-soluble degradation by-products to show evidence of degradation and to find if the by-products are non-toxic for human health and the environment. GC−MS spectra of the blank and treated samples showed ions at m/z: 30, 31, 41 43, 44, 45, 55, 57, ,58, 69, 71, 83, 85, 91 and 99. The CP-Sil 8 CB column is including 5% phenyl groups in the dimethylpolysiloxane polymer and therefore it has a slightly higher polarity than nonpolar ones such as CP-Sil 5 CB columns. This results in an improved selectivity for a wide range of compounds from polar to nonpolar ones. This column is suitable for analysis of phenols, herbicides, pesticides, amines, and so on. Using this column, the nonpolar analytes will be retained more than the polar ones, and this can be noticed from total ion current (TIC) chromatogram (Figure 5S "supplementary material") since the most nonpolar analytes were eluted later. In Table 2 we have summarized the results obtained and analysed the expected structures of the by-products. Fig. 8 shows the GC-MS spectra obtained of the water samples collected after 24 h of light exposure. The main spectrum (highest intensity) is obtained at $m/z = 45$ corresponding to the hydroxymethyl radical (Ethanolate or Ethyl alcohol). Furthermore, mass spectra obtained after prolonged exposure of 456 h is illustrated in Fig. 9. Based on m/z values in Table 2, the obtained results showed that the most abundant photocatalytic degradation by-products are ethynyloxy/acetyl radicals, hydroxypropyl, butyraldehyde, acetone, acrolein (propenal) and pentyl group. . Earlier studies on thermal degradation of PP films have reported the formation of acetaldehyde, acetic acid, acetone, formaldehyde, and a-methylacrolein as the most abundant degradation by-products (Frostling et al., 1984).

According to Hazardous Substances Data Bank (HSDB), International Agency for Research on Cancer (IARC) and National Institute of Health

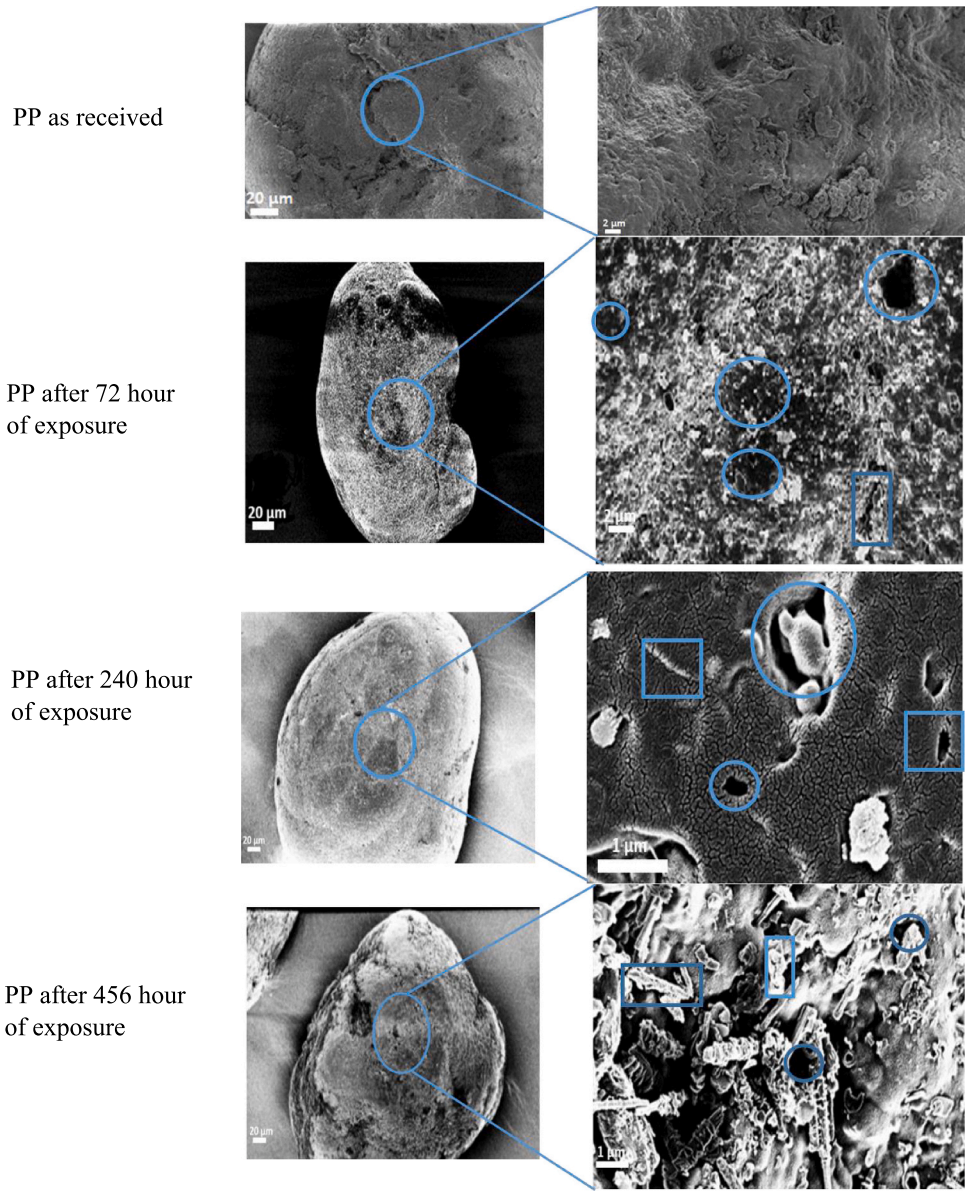

Fig. 6. SEM images of PP microplastics at different light exposure periods in the photocatalytic reactor.

(NIH), the by-products detected in water samples after photodegradation of PP microplastics may be considered to have low toxicity on human health and aquatic environment. For instance, Ethyl alcohol is widely used as a solvent and preservative in pharmaceutical preparations as well as serve as the primary ingredient in alcoholic beverages and used as a solvent of substances intended for human contact or consumption. Hydroxypropyl and acetyl groups are components of several organic compounds and pharmaceutical products. For example, hydroxypropyl cellulose is used for treatment of eye irritation. Actyl groups are a part of several well-known compounds including acetic acid and acetaminophen (paracetamol). Acetylacetone is an important commercial chemical and is used in many industrial processes as a lubricant additive, and to make colours, paints, varnishes, resins, inks, dyes, drugs, and other chemicals. Acetylacetone are used as a pesticide and it has been identified in tobacco products. Acetaldehyde is also a component of food flavourings and is added to various products, such as fruit juices and soft drinks. Its concentration in foods is generally up to 0.047% (IARC 1985). Acetone is used in the manufacturing processes of coatings, plastics, pharmaceuticals, and cosmetics. Acetone is relatively less toxic compared to many other industrial solvents (Maes et al., 2012). Acute exposures of humans to atmospheric concentrations have been reported to produce either no gross toxic effects or minor transient effects, such as eye irritation. Butyraldehyde which is found in the essential oils from flowers, fruits, leaves, and bark of various plants, is a food additive permitted for direct addition to food for human consumption as a synthetic flavouring substance.

Accumulating the structural and morphological results obtained in this work, it can thus be concluded that the FTIR (e.g., degree of oxidation), TGA, and DSC (e.g., crystallization behaviour) data analysis suggest chain scissions mechanism which was further confirmed with GC−MS analysis and that is the reason the volume of the PP microplastics particles reduces upon photodegradation as have been observed with SEM analysis. Moreover, the main photodegradation products identified by FTIR analysis (e.g., aldehydes, ketones, and alcohols) are in good agreement with the by-products determined with GC−MS. Generally, several steps may take place during the photodegradation process of PP microplastics, including initiation, propagation, chain branching, and termination. In the initial step, free radicals react with oxygen to generate hydroperoxide radical. In the case of chain branching step, the alkoxy and hydroxy radicals can be produced. Usually, the hydroperoxides are unstable species and are susceptible to decompose, that may lead to chain branching radicals. In the termination stage,

Table 1
Changes in PP microplastics particle size as a function of photocatalytic treatment for different periods of time.

Exposure Time (hour)	Particle size (µm)	Particle size distribution	Optical micrograph image
0 (as received)	154.8± 1.4	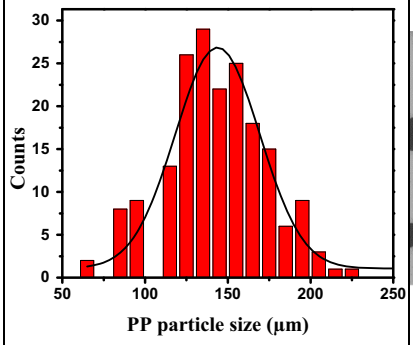	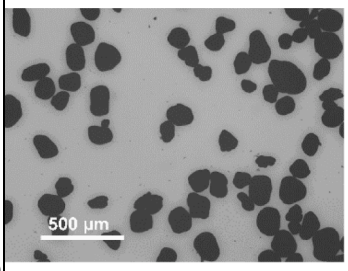
72	123.3± 0.89	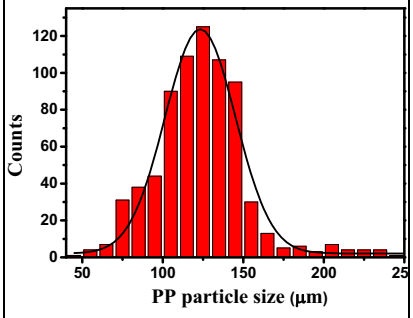	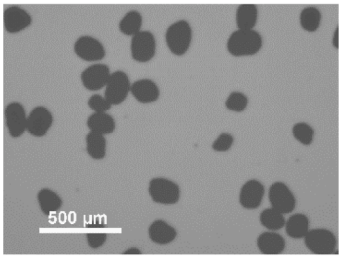
240	111.5± 0.94	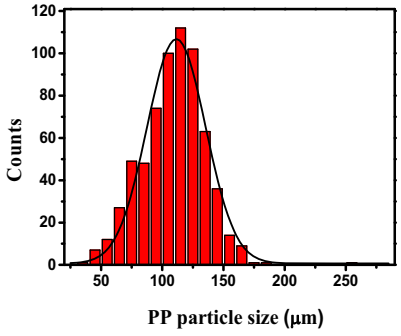	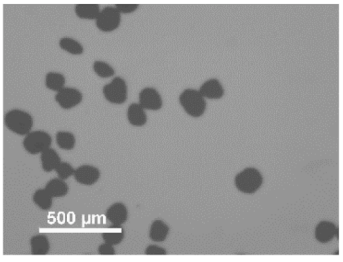
456	108.2± 2.5	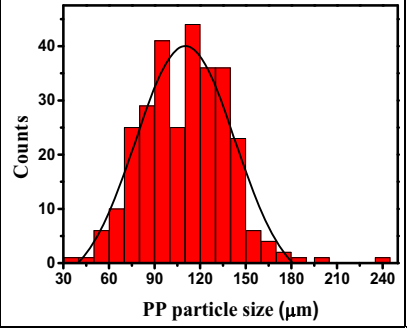	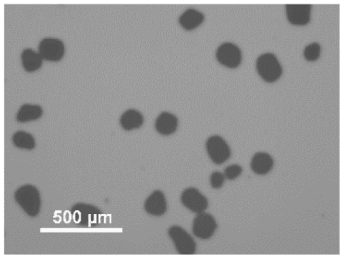

Table 2
The main photodegradation by-products of PP in water analyzed by GC/MS.

Ions (*m/z*)	Compound	Molecular formula
30	Formaldehyde	CH_2O
31	Hydroxymethyl radical	CH_3O
41	Ethynyloxy radical	C_2HO
43	Acetyl radical	CH_3CO
44	Acetaldehyde	C_2H_4O
45	Ethanolate or Ethyl alcohol radical	C_2H_5O
55	2-Propynyl, 1-hydroxy-	C_3H_3O
57	Hydroxypropyl	C_3H_5O
58	Acetone	C_3H_6O
69	2-Propenyl, 2-methyl-1-oxo-	C_4H_5O
71	Butanal (Butyraldehyde)	$CH_3CHCOCH_3$
83	4-Pentyn-1-olate	C_5H_7O
85	Hydroxypentyl	C_5H_9O
91	(2-Ethoxyethyl)oxonium	$C_4H_{11}O_2$
99	Acetylacetonate	$C_5H_7O_2$

cross-linking is a result of the reaction of different free radicals. The general photodegradation mechanism of PP microplastics is summarized as follows (Nabi et al., 2020; Verma et al., 2017; Ariza-Tarazona et al., 2020; Ohtani et al., 1989).

- The hydroxyl radicals generated from the ZnO NRs photoexcitation initiate degradation of the polymeric chains to generate PP alkyl radicals (Eq. (7)).

$$-\ CH_2CH(CH_3)CH_2\ CH(CH_3)-+\ HO^{\cdot}\rightarrow -CH_2C^{\cdot}(CH_3)CH_2CH(CH_3)- \quad (7)$$

- The propagation step involves the reaction of the alkyl radical with oxygen to form a peroxy radicals that then abstracts a hydrogen atom from another polymer chain to form a hydroperoxide (Eqs. (8) & (9)).

$$-\ CH_2C^{\cdot}(CH_3)CH_2CH(CH_3)-+O_2\rightarrow CH_2C(CH_3)(OO^{\cdot})CH_2CH(CH_3)- \quad (8)$$

$$-\ CH_2C(CH_3)(OO^{\cdot})CH_2CH(CH_3)-+-CH_2CH(CH_3)CH_2-\rightarrow\ -CH_2C(CH_3)(OOH)CH_2CH(CH_3)-+-CH_2C^{\cdot}(CH_3)CH_2- \quad (9)$$

- The formed hydroperoxide splits into two free oxy and hydroxyl radicals, by the scission of the weak $O-O$ bond (Eq. (10)).

$$-CH_2C(CH_3)(OOH)CH_2CH(CH_3)-\rightarrow\ -CH_2COCH_3-\ +C^{\cdot}H_2CH(CH_3)CH_2-\ +HO^{\cdot} \quad (10)$$

4. Conclusions

In this work, the visible light photocatalytic degradation of polypropylene microplastics was investigated using ZnO NRs coated on glass fibers in a flow through photocatalytic reactor. The FTIR results confirm efficient photodegradation of PP microplastics from appearance of carbonyl group with higher carbonyl index (CI ~ 40) after 456 h of visible light exposure, compared to reports in the literature (e.g., CI = 25 in 4200 h under UV light exposure). Fast kinetic evolution of carbonyl and hydroxyl groups are observed and the increase of the photodegradation products after 8 h of photo-irradiation becomes considerable. The degradation of PP microplastics proceed by chain scissions leading to reorganization of smaller chains as observed from the shift of crystallinity in DSC analysis and morphology in SEM analysis. Volatile organic product generation during photo-degradation produces defects in PP which are confirmed by FTIR and SEM measurements. The results obtained demonstrated that photocatalytic degradation of polypropylene microplastics continuously for two weeks under visible light (in practice considering half a day of sunlight this would be four weeks' duration) reduced its average particle volume by 65% compared to the as received polypropylene microplastics. According to several heath organizations (HSDB, IARC, NIH), in the present study the by-products detected in water samples after photodegradation of PP microplastics may considered to have low toxicity effect on human and aquatic environment. The results obtained are encouraging for a successful implementation of photocatalytic reactors for sustainable microplastics removal from water sources prior to its use or release to the environment. The increase in the photocatalytic reactor efficiency (scale-up) can be achieved by expanding the size of the device panel. Therefore, the designed reactor has a great potential for use in large-scale water and wastewater treatment.

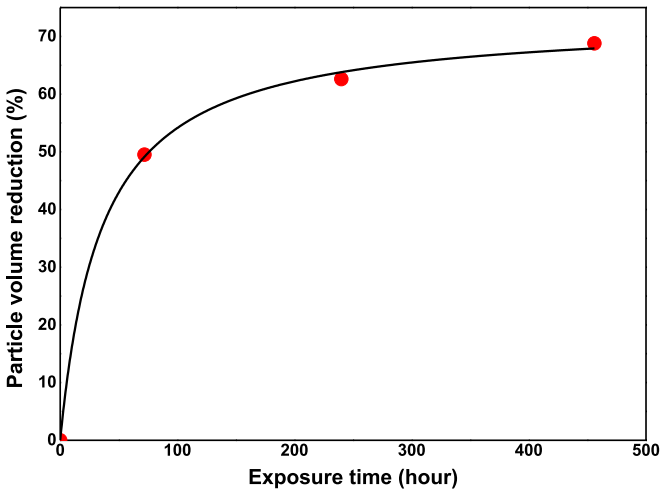

Fig. 7. The volume reduction percentage of PP microplastics particle as a function of exposure time.

CRediT authorship contributions statement

Abdusalam Uheida: Methodology, Investigation, Writing - original draft. **Hugo Giraldo Mejía:** Methodology, Writing - review & editing.

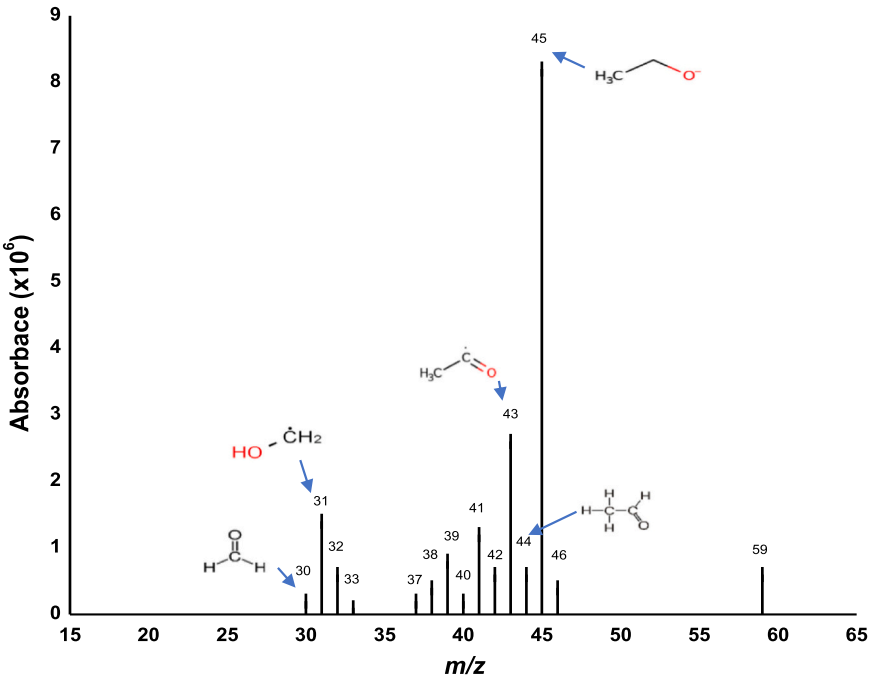

Fig. 8. GC/MS spectrum of water samples after photodegradation of PP using visible light irradiation after 24 h of irradiation. The main by-products obtained are Hydroxymethyl radical, Acetyl Radical, and Ethanolate or Ethyl alcohol radical.

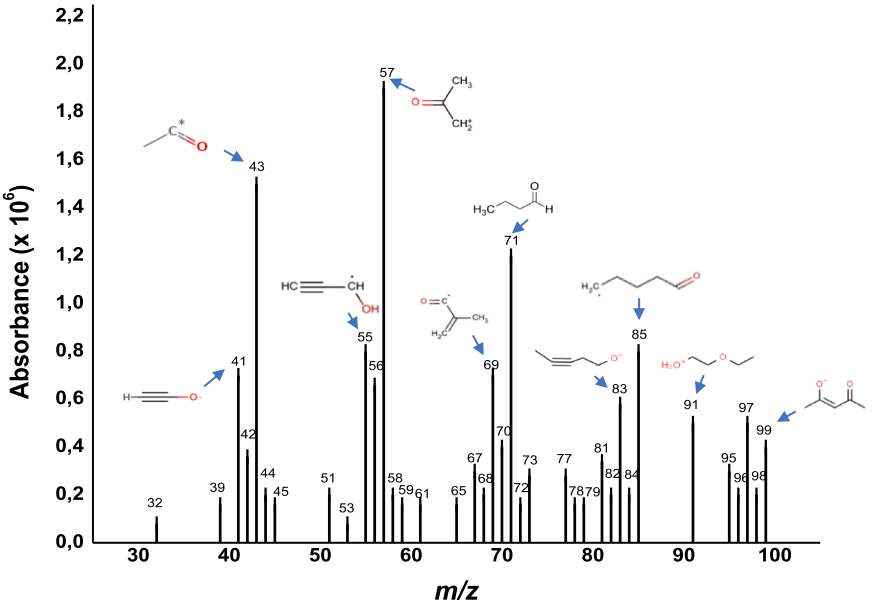

Fig. 9. GC/MS spectrum of water samples after photodegradation of PP using visible light irradiation after 456 h of irradiation. Peak identification as in Table 2. The main by-products abstained are Acetyl Radical, Hydroxypropyl, and Butyraldehyde.

Mohamed Abdel-Rehim: Formal analysis, Writing - review & editing. **Wael Hamd:** Methodology, Writing - review & editing. **Joydeep Dutta:** Conceptualization, Methodology, Writing - review & editing, Supervision.

Declaration of Competing Interest

The authors declare that they have no known competing financial interests or personal relationships that could have appeared to influence the work reported in this paper.

Acknowledgment

This work has been supported by CLAIM Project: H2020-BG-2016–2017 [grant number 774586], “Cleaning Litter by developing and Applying Innovative Methods in European seas” .

Appendix A. Supporting information

Supplementary data associated with this article can be found in the online version at doi:10.1016/j.jhazmat.2020.124299.

References

Al-Saadi, M.J., Al-Harthi, S.H., Kyaw, H.H., Myint, M.T.Z., Bora, T., Laxman, K., Al-Hinai, A., Dutta, J., 2017. Influence of atomic hydrogen, band bending, and defects in the top few nanometers of hydrothermally prepared zinc oxide nanorods. Nanoscale Res. Lett. 12, 22. https://doi.org/10.1186/s11671-016-1800-3.

Al-Sabahi, J., Bora, T., Al-Abri, M., Dutta, J., 2017. Efficient visible light photocatalysis of benzene, toluene, ethylbenzene and xylene (BTEX) in aqueous solutions using supported zinc oxide nanorods. PLoS One 12, e0189276. https://doi.org/10.1371/journal.pone.0189276.

Al-Sabahi, J., Bora, T., Al-Abri, M., Dutta, J., 2016. Controlled defects of zinc oxide nanorods for efficient visible light photocatalytic degradation of phenol. Materials (Basel) 9, 238. https://doi.org/10.3390/ma9040238.

Al-Sabahi, J., Bora, T., Claereboudt, M., Al-Abri, M., Dutta, J., 2018. Visible light photocatalytic degradation of HPAM polymer in oil produced water using supported zinc oxide nanorods. Chem. Eng. J. 351, 56–64. https://doi.org/10.1016/j.cej.2018.06.071.

Ariza-Tarazona, M.C., Villarreal-Chiu, J.F., Barbieri, V., Siligardi, C., Cedillo-González, E. I., 2019. New strategy for microplastic degradation: Green photocatalysis using a protein-based porous N-TiO_2 semiconductor. Ceram. Int. 45, 9618–9624. https://doi.org/10.1016/j.ceramint.2018.10.208.

Ariza-Tarazona, M.C., Villarreal-Chiu, J.F., Hernández-López, J.M., Rivera De la Rosa, J., Barbieri, V., Siligardi, C., Cedillo-González, E.I., 2020. Microplastic pollution reduction by a carbon and nitrogen-doped TiO_2: effect of pH and temperature in the photocatalytic degradation process. J. Hazard. Mater. 395, 122632 https://doi.org/10.1016/j.jhazmat.2020.122632.

Arutchelvi, J., Sudhakar, M., Arkatkar, A., Doble, M., Bhaduri, S., Uppara, P.V., 2008. Biodegradation of polyethylene and polypropylene. doi: 10.1016/j.scitotenv.2019.134125.

Ashri, N.Y., Abdel-Rehim, M., 2011. Sample treatment based on extraction techniques in biological matrices. Bioanalysis 3, 2003–2018. https://doi.org/10.4155/bio.11.201.

Aslanzadeh, S., Haghighat Kish, M., 2010. Photo-oxidation of polypropylene fibers exposed to short wavelength UV radiations. Fibers Polym. 11, 710–718. https://doi.org/10.1007/s12221-010-0710-8.

Auta, H.S., Emenike, C.U., Fauziah, S.H., 2017. Screening of Bacillus strains isolated from mangrove ecosystems in Peninsular Malaysia for microplastic degradation. Environ. Pollut. 231, 1552–1559. https://doi.org/10.1016/j.envpol.2017.09.043.

Baruah, S., Dutta, J., 2009. Hydrothermal growth of ZnO nanostructures. Sci. Technol. Adv. Mater. 10, 013001 https://doi.org/10.1088/1468-6996/10/1/013001.

Baruah, S., Dutta, J., 2009. pH-dependent growth of zinc oxide nanorods. J. Cryst. Growth 311, 2549–2554. https://doi.org/10.1016/j.jcrysgro.2009.01.135.

Baruah, S., Dutta, J., 2009. Effect of seeded substrates on hydrothermally grown ZnO nanorods. J. Sol. Gel. Sci. Technol. 50, 456–464. https://doi.org/10.1007/s10971-009-1917-2.

Baruah, S., Jaisai, M., Dutta, J., 2012. Development of a visible light active photocatalytic portable water purification unit using ZnO nanorods. Catal. Sci. Technol. 2, 918. https://doi.org/10.1039/C2CY20033C.

Baruah, S., Mahmood, M.A., Myint, M.T.Z., Bora, T., Dutta, J., 2010. Enhanced visible light photocatalysis through fast crystallization of zinc oxide nanorods. Beilstein J. Nanotechnol. 1, 14–20. https://doi.org/10.3762/bjnano.1.3.

Baruah, S., Rafique, R.F., Dutta, J., 2008. Visible light photocatalysis by tailoring crystal defects in zinc oxide nanostructures. Nano 03, 399–407. https://doi.org/10.1142/S179329200800126X.

Bora, T., Sathe, P., Laxman, K., Dobretsov, S., Dutta, J., 2017. Defect engineered visible light active ZnO nanorods for photocatalytic treatment of water. Catal. Today 284, 11–18. https://doi.org/10.1016/j.cattod.2016.09.014.

Bora, T., Zoepfl, D., Dutta, J., 2016. Importance of plasmonic heating on visible light driven photocatalysis of gold nanoparticle decorated zinc oxide nanorods. Sci. Rep. 6, 26913 https://doi.org/10.1038/srep26913.

Bratovcic, A., 2019. Degradation of micro-and nano-plastics by photocatalytic methods. J. Nanosci. Nanotechnol. Appl. 3, 304–309. https://doi.org/10.18875/2577-7920.3.304.

Browne, M.A., Crump, P., Niven, S.J., Teuten, E., Tonkin, A., Galloway, T., Thompson, R., 2011. Accumulation of microplastic on shorelines woldwide: sources and sinks. Environ. Sci. Technol. 45, 9175–9179. https://doi.org/10.1021/es201811s.

Burns, E.E., Boxall, A.B.A., 2018. Microplastics in the aquatic environment: Evidence for or against adverse impacts and major knowledge gaps. Environ. Toxicol. Chem. 37, 2776–2796. https://doi.org/10.1002/etc.4268.

Canopoli, L., Coulon, F., Wagland, S.T., 2020. Degradation of excavated polyethylene and polypropylene waste from landfill. Sci. Total Environ. 698, 134125 https://doi.org/10.1016/j.scitotenv.2019.134125.

de Carvalho, C.L., Silveira, A.F., Rosa, D.D.S., 2013. A study of the controlled degradation of polypropylene containing pro-oxidant agents. Springerplus 2, 623. https://doi.org/10.1186/2193-1801-2-623.

Chang, M., 2015. Reducing microplastics from facial exfoliating cleansers in wastewater through treatment versus consumer product decisions. Mar. Pollut. Bull. 101, 330–333. https://doi.org/10.1016/j.marpolbul.2015.10.074.

Cox, K.D., Covernton, G.A., Davies, H.L., Dower, J.F., Juanes, F., Dudas, S.E., 2019. Human consumption of microplastics. Environ. Sci. Technol. 53, 7068–7074. https://doi.org/10.1021/acs.est.9b01517.

Davis, T.E., Tobias, R.L., Peterli, E.B., 1962. Thermal degradation of polypropylene. J. Polym. Sci. 56, 485–499. https://doi.org/10.1002/pol.1962.1205616420.

Dobretsov, S., Sathe, P., Bora, T., Barry, M., Myint, M.T.Z., Abri, M.A., 2020. Toxicity of different zinc oxide nanomaterials at 3 trophic levels: implications for development of low-toxicity antifouling agents. Environ. Toxicol. Chem. 39, 1343–1354. https://doi.org/10.1002/etc.4720.

El-Dessouky, H.M., Lawrence, C.A., 2010. Nanoparticles dispersion in processing functionalised PP/TiO_2 nanocomposites: distribution and properties. J. Nanopart. Res. 13, 1115–1124. https://doi.org/10.1007/s11051-010-0100-6.

Enfrin, M., Dumée, L.F., Lee, J., 2019. Nano/microplastics in water and wastewater treatment processes – origin, impact and potential solutions. Water Res. 161, 621–638. https://doi.org/10.1016/j.watres.2019.06.049.

Fendall, L.S., Sewell, M.A., 2009. Contributing to marine pollution by washing your face: microplastics in facial cleansers. Mar. Pollut. Bull. 58, 1225–1228. https://doi.org/10.1016/j.marpolbul.2009.04.025.

Fonseca, M.M.A., Gamarro, E.G., Toppe, J., Bahri, T., Barg, U., 2017. The Impact of Microplastics on Food Safety: the Case of Fishery and Aquaculture Products. FAO Aquaculture Newsletter 43–45. ⟨www.fao.org/publications⟩.

Frostling, H., Hoff, A., Jacobsson, S., Pfaffli, P., Vainiotalo, S., Zitting, A., 1984. Analytical, occupational and toxicologic aspects of the degradation products of polypropylene plastics. Scand. J. Work Environ. Health 10, 163–169. https://doi.org/10.5271/sjweh.2347.

García-Montelongo, X.L., Martínez-de la Cruz, A., Vázquez-Rodríguez, S., Torres-Martínez, L.M., 2014. Photo-oxidative degradation of TiO_2/polypropylene films. Mater. Res. Bull. 51, 56–62. https://doi.org/10.1016/j.materresbull.2013.11.040.

Jambeck, J.R., Geyer, R., Wilcox, C., Siegler, T.R., Perryman, M., Andrady, A., Narayan, R., Law, K.L., 2015. Plastic waste inputs from land into the ocean. Science 347, 768–771. https://doi.org/10.1126/science.1260352.

Kamrannejad, M.M., Hasanzadeh, A., Nosoudi, N., Mai, L., Babaluo, A.A., 2014. Photocatalytic degradation of polypropylene/TiO_2 nano-composites. Mater. Res. 17, 1039–1046. https://doi.org/10.1590/1516-1439.267214.

Llorente-García, B.E., Hernández-López, J.M., Zaldívar-Cadena, A.A., Siligardi, C., Cedillo-González, E.I., 2020. First insights into photocatalytic degradation of HDPE and LDPE microplastics by a mesoporous N–TiO_2 coating: effect of size and shape of microplastics. Coatings 10, 658. https://doi.org/10.3390/coatings10070658.

Maes, J., Verlooy, L., Buenafe, O.E., de Witte, P.A.M., Esguerra, C.V., Crawford, A.D., 2012. Evaluation of 14 organic solvents and carriers for screening applications in zebrafish embryos and larvae. PLoS One 7, e43850. https://doi.org/10.1371/journal.pone.0043850.

Murphy, F., Ewins, C., Carbonnier, F., Quinn, B., 2016. Wastewater treatment works (WwTW) as a source of microplastics in the aquatic environment. Environ. Sci. Technol. 50, 5800–5808. https://doi.org/10.1021/acs.est.5b05416.

Nabi, I., Bacha, A.-U.-R., Li, K., Cheng, H., Wang, T., Liu, Y., Ajmal, S., Yang, Y., Feng, Y., Zhang, L., 2020. Complete photocatalytic mineralization of microplastic on TiO_2 nanoparticle film. iScience 23, 101326. https://doi.org/10.1016/j.isci.2020.101326.

Nakata, K., Fujishima, A., 2012. TiO_2 photocatalysis: design and applications. J. Photochem. Photobiol. C Photochem. Rev. 13, 169–189. https://doi.org/10.1016/j.jphotochemrev.2012.06.001.

Ohtani, B., Adzuma, S., Miyadzu, H., Nishimoto, S.-i, Kagiya, T., 1989. Photocatalytic degradation of polypropylene film by dispersed titanium dioxide particles. Polym. Degrad. Stab. 23, 271–278. https://doi.org/10.1016/0141-3910(89)90101-8.

Promnimit, S., Baruah, S., Lamdu, U., Dutta, J., 2012. Hydrothermal growth of ZnO hexagonal nanocrystals: effect of growth conditions. J. Nano Res. 21, 57–63. https://doi.org/10.4028/www.scientific.net/JNanoR.21.57.

Rabello, M.S., White, J.R., 1997. Photodegradation of polypropylene containing a nucleating agent. J. Appl. Polym. Sci. 64, 2505–2517. https://doi.org/10.1002/(SICI)1097-4628(19970627)64:13<2505::AID-APP4>3.0.CO;2-H.

Rånby, B., 1989. Photodegradation and photo-oxidation of synthetic polymers. J. Anal. Appl. Pyrolysis 15, 237–247. https://doi.org/10.1016/0165-2370(89)85037-5.

Redondo-Hasselerharm, P.E., Gort, G., Peeters, E.T.H.M., Koelmans, A.A., 2020. Nano- and microplastics affect the composition of freshwater benthic communities in the long term. Sci. Adv. 6, eaay4054 https://doi.org/10.1126/sciadv.aay4054.

Rouillon, C., Bussiere, P.O., Desnoux, E., Collin, S., Vial, C., Therias, S., Gardette, J.L., 2016. Is carbonyl index a quantitative probe to monitor polypropylene photodegradation? Polym. Degrad. Stab. 128, 200–208. https://doi.org/10.1016/j.polymdegradstab.2015.12.011.

Scientific opinion on the safety evaluation of the substance zinc oxide, nanoparticles, uncoated and coated with [3–(methacryloxy)propyl] trimethoxysilane, for use in food contact materials. EFSA J. 13, 2015. https://doi.org/10.2903/j.efsa.2015.4063.

Silva, A.B., Costa, M.F., Duarte, A.C., 2018. Biotechnology advances for dealing with environmental pollution by micro(nano)plastics: lessons on theory and practices. Curr. Opin. Environ. Sci. Health 1, 30–35. https://doi.org/10.1016/j.coesh.2017.10.005.

Sol, D., Laca, A., Laca, A., Díaz, M., 2020. Approaching the environmental problem of microplastics: importance of WWTP treatments. Sci. Total Environ. 740, 140016 https://doi.org/10.1016/j.scitotenv.2020.140016.

Talvitie, J., Mikola, A., Setälä, O., Heinonen, M., Koistinen, A., 2017. How well is microlitter purified from wastewater? – a detailed study on the stepwise removal of microlitter in a tertiary level wastewater treatment plant. Water Res. 109, 164–172. https://doi.org/10.1016/j.watres.2016.11.046.

Tofa, T.S., Kunjali, K.L., Paul, S., Dutta, J., 2019a. Visible light photocatalytic degradation of microplastic residues with zinc oxide nanorods. Environ. Chem. Lett. 17, 1341–1346. https://doi.org/10.1016/j.enmm.2016.01.001.

Tofa, T.S., Ye, F., Kunjali, K.L., Dutta, J., 2019b. Enhanced visible light photodegradation of microplastic fragments with plasmonic platinum/zinc oxide nanorod photocatalysts. Catalysts 9, 819. https://doi.org/10.3390/catal9100819.

Torikai, A., Suzuki, K., Fueki, K., 1983. Photodegradation of polypropylene and polypropylene containing pyrene. Polym. Photochem. 3, 379–390. https://doi.org/10.1016/0144-2880(83)90051-9.

Verma, R., Singh, S., Dalai, M.K., Saravanan, M., Agrawal, V.V., Srivastava, A.K., 2017. Photocatalytic degradation of polypropylene film using TiO_2-based nanomaterials

under solar irradiation. Mater. Des. 133, 10–18. https://doi.org/10.1016/j.matdes.2017.07.042.
White, J.R., Shyichuk, A.V., Turton, T.J., Syrotynska, I.D., 2006. Effect of stabilizer and pigment on photodegradation of polypropylene as revealed by macromolecule scission and crosslinking measurements. Polym. Degrad. Stab. 91, 1755–1760. https://doi.org/10.1016/j.polymdegradstab.2005.11.017.
Wright, S.L., Kelly, F.J., 2017. Plastic and human health: a micro issue? Environ. Sci. Technol. 51, 6634–6647. https://doi.org/10.1021/acs.est.7b00423.
Yang, C.Q., Martin, L.K., 1994. Photo- and thermal-oxidation of the nonwoven polypropylene fabric studied by FT-IR photoacoustic spectroscopy. J. Appl. Polym. Sci. 51, 389–397. https://doi.org/10.1002/app.1994.070510301.
Zhao, X., Li, Z., Chen, Y., Shi, L., Zhu, Y., 2007. Solid-phase photocatalytic degradation of polyethylene plastic under UV and solar light irradiation. J. Mol. Catal. A Chem. 268, 101–106. https://doi.org/10.1016/j.molcata.2006.12.012.
Zhao, H., Li, R.K.Y., 2006. A study on the photo-degradation of zinc oxide (ZnO) filled polypropylene nanocomposites. Polymer 47, 3207–3217. https://doi.org/10.1016/j.polymer.2006.02.089.